

UC Berkeley

UC Berkeley Previously Published Works

Title

Nuclear physics without high-momentum potentials: Constructing the nuclear effective interaction directly from scattering observables

Permalink

<https://escholarship.org/uc/item/29c6h3dj>

Authors

McElvain, KS
Haxton, WC

Publication Date

2019-10-01

DOI

10.1016/j.physletb.2019.134880

Peer reviewed



Nuclear physics without high-momentum potentials: Constructing the nuclear effective interaction directly from scattering observables



K.S. McElvain ^{a,b,*}, W.C. Haxton ^{a,b}

^a Department of Physics, University of California, Berkeley, CA, USA

^b Lawrence Berkeley National Laboratory, Berkeley, CA, USA

ARTICLE INFO

Article history:

Received 17 February 2019
 Received in revised form 13 July 2019
 Accepted 20 August 2019
 Available online 28 August 2019
 Editor: J.-P. Blaizot

Keywords:

Effective theory
 Nucleon-nucleon interaction
 Phase shifts

ABSTRACT

The traditional approach to nuclear physics encodes phase shift information in a nucleon-nucleon (NN) potential, producing a nucleon-level interaction that captures the sub-GeV consequences of QCD. A further reduction to the nuclear scale is needed to produce an effective interaction for soft Hilbert spaces, such as those employed in the shell model. Here we describe an alternative construction of the effective interaction that is simple and quite precise, proceeding from the QCD scale directly to the nuclear scale. This eliminates the need for constructing and renormalizing the high-momentum NN potential. Instead, continuum phase shifts and mixing angles are used directly at the nuclear scale. The method exploits the analytic continuity in energy of HOBET (Harmonic-Oscillator-Based Effective Theory) to connect bound states to continuum solutions at specific energies. The procedure is systematic, cutoff independent, and convergent, yielding keV accuracy at NNLO or N³LO, depending on the channel. Lepage plots are provided.

© 2019 The Author(s). Published by Elsevier B.V. This is an open access article under the CC BY license (<http://creativecommons.org/licenses/by/4.0/>). Funded by SCOAP³.

The traditional approach to nuclear physics employs an NN potential to encode experimental phase shift information, which is then renormalized to produce an effective interaction appropriate for soft, discrete bases, such as those used in the shell model (SM). Most often NN potentials (see [1–4]) are determined empirically. For example, the Argonne v_{18} interaction [2,3] contains 18 operator components and 40 parameters, adjusted to reproduce pp and np scattering data over the energy range 0–350 MeV, as well as low energy nn scattering parameters and the deuteron binding energy. Phenomenological forms are assumed for the associated short- and mid-ranged radial forms, including correlation functions that build in hard cores at $r \sim 0.5$ fm.

Chiral effective field theory (EFT) provides an alternative to such phenomenologically derived NN potentials (see the reviews [5,6] and references therein). As a systematic expansion, chiral EFT provides a basis for error estimation and for the systematic inclusion of three- and other multi-nucleon interactions [7], including the order at which these become important in a given counting scheme. The starting point is an effective Lagrangian with pion and nucleon fields, and often including an explicit delta. Physics above the break-down scale $\Lambda_b \sim 1 \text{ GeV} \sim m_\rho$ is represented through

short-range effective operators, with good convergence expected for momenta q where $\frac{q}{\Lambda_b} \ll 1$. Typically such potentials are regulated, as otherwise the introduction of counterterms to guarantee the convergence of loops becomes tedious.

Both approaches encode experimental scattering data in an NN potential, which then must be renormalized to produce an interaction appropriate for SM-like soft spaces. This two-step renormalization procedure – the introduction of a GeV-scale nucleon-level effective theory (ET) in the guise of an NN potential, then integrating out most of the high momentum content of that potential in forming a soft nuclear effective interaction – is somewhat unusual. In other EFT contexts the reduction is done in one step, from the initial ultraviolet (UV) theory directly to the desired P (or included) space (here the SM space). One identifies the general form of the effective interaction in P based on a relevant operator expansion, then determines the coefficients of these operators (the low-energy constants or LECs) by matching to observables.

The nuclear two-step procedure is tricky to execute well, in part because the natural bases for describing the NN interaction and multi-nucleon bound states have different properties. As NN interactions are determined from phase shifts, the natural basis consists of continuum plane-wave states. In contrast, the only discrete and compact Hilbert space available for describing translationally invariant bound states is the harmonic oscillator (HO): P spaces containing a complete set of HO Slater determinants of energy

* Corresponding author.

E-mail addresses: kemcelvain@berkeley.edu (K.S. McElvain), haxton@berkeley.edu (W.C. Haxton).

$E \leq \Lambda_{SM} \hbar \omega$ (relative to the naive ground state) can be exactly separated into center-of-mass (CM) and relative motion. Separability of the Hilbert space, while perhaps not an overriding concern in models, is crucial in an EFT, as it leads to a translationally invariant effective interaction, a great simplification. The resulting lack of orthogonality between NN (plane wave) and nuclear (HO) bases limit the extent to which the NN potential can be softened by methods discussed below, forcing one to deal with at least a semi-hard core in the subsequent nuclear effective interactions step.

Early attempts to solve the effective interactions problem quantitatively were typically diagrammatic: the nuclear reaction matrix G was approximated by perturbing in the bare two-nucleon reaction matrix G_0 [8], generating intermediate particle-hole excitations [9]. This approach was found to fail in the early 1970s. Barrett and Kirson [10], working in a SM basis, evaluated the effective interaction for ^{18}F , finding large third-order contributions to G that tended to cancel against second-order contributions. At about the same time Shucan and Weidenmuller [11,12] identified the presence of intruder states – states of the full Hamiltonian that appear within the spectrum of P , but reside primarily outside of P – as a generic source of such nonperturbative behavior.

In another early approach, phenomenological super-soft potentials [13,14] were sought in order to make the nuclear renormalization step more tractable. This idea has modern but more systematic analogs in which a high-momentum NN potential is softened, while not losing physics important to P . A modest reduction of a potential's cutoff scale Λ can have great impact on the numerical complexity of the effective interactions problem: the number of single-particle states should diminish as Λ^3 , while the dimension of the A -body Hilbert space depends combinatorially on the single-particle basis size [15]. Two procedures widely applied are the $V_{\text{low } k}$ [16–20] and the similarity renormalization group (SRG) [21–24]. In the SRG approach a continuous sequence of unitary transformations $\hat{U}(s)$ are applied to the Hamiltonian, indexed by a continuous flow parameter s , with the variation in s generating a flow equation which can be exploited to decouple the excluded space from the included space P . The procedure has been carried out in free space but also with respect to an in-medium reference state [25]. In the $V_{\text{low } k}$ approach the T matrix for a potential $V_{NN}^{\Lambda_\infty}$ characterized by a high momentum cutoff Λ_∞ is matched to one for a low-momentum potential $V_{\text{low } k}^\Lambda$ characterized by a lower cutoff Λ . The matching is done, preserving either the full off-shell or the half-on-shell T matrix. In the procedure followed in [20], based on [26], a discretization step employing a finite set of eigenvectors is used to first transform to a momentum-dependent non-Hermitian Hamiltonian, and then into a Hermitian form via a Okubo transformation. The $V_{\text{low } k}$ and SRG procedures have the attractive property of integrating out the more model-dependent, short-range behavior of potentials, putting them into a nearly universal form.

These methods have been used with good success to lower cutoffs scales to $\Lambda \sim 2 \text{ fm}^{-1} \sim 400 \text{ MeV}$. Problems arise if Λ is reduced further, cutting into momentum scales important to typical SM [27–29] and coupled cluster [30,31] P spaces: one must retain in the softened potential all Fourier components that are numerically significant within P . As these procedures are typically executed at the NN level, another issue is the omission of three- and higher-body corrections that grow in importance as Λ is lowered. In coupled cluster calculations using $V_{\text{low } k}^\Lambda$, significant variations in the ground state energies of ^{16}O , ^{15}O , and ^{15}N with cutoff, $1.6 \leq \Lambda \leq 2.2 \text{ fm}^{-1}$, have been interpreted as indicating the importance of omitted three-body terms [32].

Such softened potentials greatly help, but still leave a challenging renormalization step to reach P . Here we describe a direct, one-step procedure for calculating the effective interaction appro-

priate for nuclear calculations in translationally invariant HO P spaces. The scattering data that normally are encoded in a high-momentum potential are instead used to determine the effective interaction's LECs. The only cutoffs or regulators in the treatment are those defined by P itself (the oscillator parameter b and Λ_{SM}). While the choice of b and Λ_{SM} can affect the rate of convergence, converged results are independent of whatever choice is made. The theory, which comes in pionless and pionful forms, is highly convergent, with keV accuracy achieved in NNLO or N^3LO , depending on the channel.

HOBET [33–37], uses the energy-dependent Bloch-Horowitz (BH) equation [38] to generate the effective interaction within a finite HO P space. The BH equation produces exact eigenvalues and exact restrictions of the true wave functions Ψ to P . This attractive definition of effective wave functions as restrictions to P is a consequence of the energy dependence: as projection onto P does not preserve scalar products, this property cannot be achieved with Hermitian energy-independent effective Hamiltonians. BH solutions evolve simply with increases in Λ_{SM} , with new components added but old components unchanged. Another attractive consequence of the energy dependence is the generation of every eigenstate having a nonzero overlap with P (in general, an infinite number) even though the Hilbert space P is finite. Consequently intruder states mixing into P are included in BH treatments: even if a state resides almost entirely in Q , it will be generated at the proper energy in a BH treatment, with the proper mixing into P , constrained by the fit we do to phase shift data, which is performed continuously in E .

Despite these attractive properties of BH solutions, there is some prejudice against energy-dependent approaches in nuclear physics [15,39]. As was originally demonstrated by Brandow [40] via folded diagrams, the energy dependence can be removed to yield an energy-independent, non-Hermitian Hamiltonian that preserves the attractive properties of BH equation solutions. But more commonly a form of the Lee-Suzuki [41,42] transformation is employed to produce an energy-independent Hermitian interaction reproducing certain eigenvalues, but not the other properties described above.

From the perspective of ET, energy-dependent formulations have another attractive property, preserving analytic continuity in energy important to describing both bound and continuum states seamlessly. Most of the information carried by NN phase shifts is encoded in their evolution with energy, which is especially rapid near threshold. In an ET that keeps energy an explicit parameter, this information can be used directly and simply.

There are reasons one can offer for eschewing energy-dependent approaches. One is the need to find self-consistent solutions of the BH equation: the eigenvalue sought appears as a parameter in the effective interaction used. But in HOBET calculations performed to date [33–37], energy self-consistency to machine accuracy is achieved very quickly by iteration, typically in 5-6 steps. It is possible to organize the algorithm so that steps after the first require little work. Second and perhaps more serious is the assumption that the LECs of an energy-dependent formulation must themselves depend on energy – one envisions a BH effective interaction resembling Argonne v_{18} , except that a distinct set of 40 parameters would be needed at every energy. Such complexity could easily convince one to seek a different approach.

Key to resolving the second issue is the observation that an ET formulated in a finite HO basis requires corrections in both the UV and infrared (IR), the former because the hard core is unresolved in P , the latter because the HO over-confines weakly bound nuclear states. UV corrections are associated with hard short-range scattering that kicks nucleons high into the excluded space $Q = 1 - P$: differences in energies of the initial states in P are of little con-

sequence. In contrast, IR corrections are governed by the relative kinetic energy operator T , a ladder operator in the HO that couples the last included shell in P with the first excluded shell of the same parity in Q : the lack of any scale separation in the IR leads to sharp energy dependence and also very slow convergence of IR corrections in perturbation theory [34,35]. The IR is responsible for $\sim 95\%$ of the nuclear BH equation's energy dependence.

These observations motivated the following reorganization of the BH equation to separate IR and UV corrections [34,35].

$$\begin{aligned} PH^{\text{eff}}P|\Psi\rangle &= EP|\Psi\rangle, \\ G_{QT} &\equiv \frac{1}{E - QT}, \quad G_{QH} \equiv \frac{1}{E - QH}, \quad H \equiv T + V, \\ H^{\text{eff}} &= EG_{TQ}(E) \left[T + T \frac{Q}{E} T + V + V_{\delta} \right] EG_{QT}(E), \\ &VG_{QH}QV \leftrightarrow V_{\delta}. \end{aligned} \quad (1)$$

This reorganization yields Green's functions in QT that carry almost all of the energy dependence. The QT summation to all orders nonperturbatively incorporates into H^{eff} the IR physics missing from P [34,35]. In [37] it was shown that V_{δ} can be readily represented by a contact-gradient expansion with constant LECs, thereby encoding the nonperturbative effects of the UV physics missing from P . Any residual energy dependence not captured by the Green's functions is easily absorbed by the associate operators. Consequently $H^{\text{eff}}(E)$'s LEC parameterization is as simple as that of standard NN potentials. In [37] those LECs were determined from the Argonne v_{18} by numerical renormalization. Here we will show they can be determined directly, without the use of an NN potential, from the variation of phase shifts with energy.

Numerical solutions of Eq. (1) for two- and three-nucleon systems can be obtained for bound or continuum states in formulations that begin with a potential V [34,35,37]. Such solutions exhibit all of the BH equation properties described above. We discuss the three contributions to Eq. (1), V_{δ} , V , and the kinetic energy, in turn.

HOBET's short-range expansion for V_{δ} [37] is built on the HO creation operators $(a_x^{\dagger}, a_y^{\dagger}, a_z^{\dagger}) \equiv a_i^{\dagger}$ and their conjugates

$$a_i^{\dagger} \equiv \frac{1}{\sqrt{2}} \left(-\frac{\partial}{\partial r_i} + r_i \right), \quad a_i \equiv \frac{1}{\sqrt{2}} \left(\frac{\partial}{\partial r_i} + r_i \right),$$

which satisfy the usual commutation relations. Here $\mathbf{r} = (\mathbf{r}_1 - \mathbf{r}_2)/\sqrt{2}b$ is the dimensionless Jacobi coordinate. Defining projections with good angular momentum, $a_M^{\dagger} = \hat{\mathbf{e}}_M \cdot \mathbf{a}^{\dagger}$ and $\tilde{a}_M = (-1)^{M+1} a_{-M}$, where $\hat{\mathbf{e}}_M$ is the spherical unit vector, we can form the scalar HO nodal raising/lowering operators $\hat{A}^{\dagger} \equiv \mathbf{a}^{\dagger} \odot \mathbf{a}^{\dagger}$, $\hat{A} \equiv \tilde{\mathbf{a}} \odot \tilde{\mathbf{a}}$

$$\hat{A} |n\ell m\rangle = -2 \sqrt{(n-1)(n+\ell-1/2)} |n-1 \ell m\rangle,$$

where $|n\ell m\rangle$ is a normalized HO state. Using

$$\begin{aligned} \delta(\mathbf{r}) &= \sum_{n'n} d_{n'n} |n'00\rangle \langle n00|, \\ d_{n'n} &\equiv \frac{2}{\pi^2} \left[\frac{\Gamma(n'+\frac{1}{2})\Gamma(n+\frac{1}{2})}{(n'-1)!(n-1)!} \right]^{1/2}, \end{aligned} \quad (2)$$

HOBET's short-range expansion can be carried out, which we note below is a Talmi moment expansion about the momentum scale b^{-1} [37]. We obtain for the 1S_0 channel $N^3\text{LO}$ interaction

$$\begin{aligned} V_{\delta}^S &= \sum_{n'n} d_{n'n} \left[a_{LO}^S |n'0\rangle \langle n0| \right. \\ &+ a_{NLO}^S \left\{ \hat{A}^{\dagger} |n'0\rangle \langle n0| + |n'0\rangle \langle n0| \hat{A} \right\} \\ &+ a_{NNLO}^{S,22} \hat{A}^{\dagger} |n'0\rangle \langle n0| \hat{A} \\ &+ a_{NNLO}^{S,40} \left\{ (\hat{A}^{\dagger})^2 |n'0\rangle \langle n0| + |n'0\rangle \langle n0| \hat{A}^2 \right\} \\ &+ a_{N^3LO}^{S,42} \left\{ \hat{A}^{\dagger 2} |n'0\rangle \langle n0| \hat{A} + \hat{A}^{\dagger} |n'0\rangle \langle n0| \hat{A}^2 \right\} \\ &+ a_{N^3LO}^{S,60} \left\{ \hat{A}^{\dagger 3} |n'0\rangle \langle n0| + |n'0\rangle \langle n0| \hat{A}^3 \right\} \left. \right], \end{aligned} \quad (3)$$

where the LECs a_{LO}, a_{NLO}, \dots carry units of energy. The HO matrix elements are

$$\begin{aligned} \langle n'(\ell' = 0S)JM|V_{\delta}^S|n(\ell = 0S)JM\rangle &= d_{n'n} \left[\right. \\ &a_{LO}^S - 2[(n'-1) + (n-1)]a_{NLO}^S + 4(n'-1)(n-1)a_{NNLO}^{S,22} \\ &+ 4((n'-1)(n'-2) + (n-1)(n-2))a_{NNLO}^{S,40} \\ &- 8((n'-1)(n'-2)(n-1) + (n'-1)(n-1)(n-2))a_{N^3LO}^{S,42} \\ &\left. - 8((n'-1)(n'-2)(n'-3) + (n-1)(n-2)(n-3))a_{N^3LO}^{S,60} \right] \end{aligned} \quad (4)$$

In tensor channels, such as 3S_1 - 3D_1 the angular momentum raising and lowering operators are needed, formed from the fully aligned coupling of the spherical creation and annihilation operators

$$\begin{aligned} \langle n\ell || \left[\mathbf{a}^{\dagger} \otimes \dots \otimes \mathbf{a}^{\dagger} \right]_{\ell} || n0\rangle &= \langle n0 || \left[\tilde{\mathbf{a}} \otimes \dots \otimes \tilde{\mathbf{a}} \right]_{\ell} || n\ell\rangle = \\ &2^{\ell/2} \sqrt{\frac{l!}{(2\ell-1)!!} \frac{\Gamma[n+\ell+\frac{1}{2}]}{\Gamma[n+\frac{1}{2}]}} \end{aligned} \quad (5)$$

where $||$ denotes a reduced matrix element. By applying the angular momentum raising operator to the delta function expansion one can form operators such as

$$\begin{aligned} V_{\delta}^{\text{SD}} &= \sum_{n'n} d_{n'n} \left[a_{NLO}^{\text{SD}} \left\{ \left[\mathbf{a}^{\dagger} \otimes \mathbf{a}^{\dagger} \right]_2 |n'0\rangle \langle n0| + \right. \right. \\ &\left. \left. |n'0\rangle \langle n0| \left[\tilde{\mathbf{a}} \otimes \tilde{\mathbf{a}} \right]_2 \right\} \odot \left[\sigma_1 \otimes \sigma_2 \right]_2 + \dots \right]. \end{aligned} \quad (6)$$

Full results through $N^3\text{LO}$ for all contributing channels can be found in [37].

Equation (4) shows that HOBET's ladder operator expansion generates a characteristic dependence on nodal quantum numbers n, n' : a_{LO}^S is the only LEC contributing to the HO $1s$ - $1s$ ($n = n' = 1$) matrix element, a_{NLO}^S is the only additional LEC contributing to the $1s$ - $2s$ matrix element, etc. Consequently if one starts with an NN potential – the two-step process described previously for either a hard potential like Argonne v_{18} or a softer one like $V_{\text{low } k}$ – the LECs can be fixed in a scheme-independent way, once one computes individual matrix elements of the effective interaction. If a_{LO}^S is determined from the $1s$ - $1s$ matrix element in a LO calculation, that value will not change at NLO, and so on. The s -wave LECs in this scheme are proportional to

$$\int r'^2 dr' r^2 dr r'^{2(n'-1)} e^{-r'^2/2} V_Q(r', r) r^{2(n-1)} e^{-r^2/2}, \quad (7)$$

with $V_Q \sim VG_{QH}QV$: this identifies the LECs as a nonlocal generalization of Talmi integrals [43]. In [37] the Talmi integral correspondence with LECs was used to demonstrate that the hierarchy

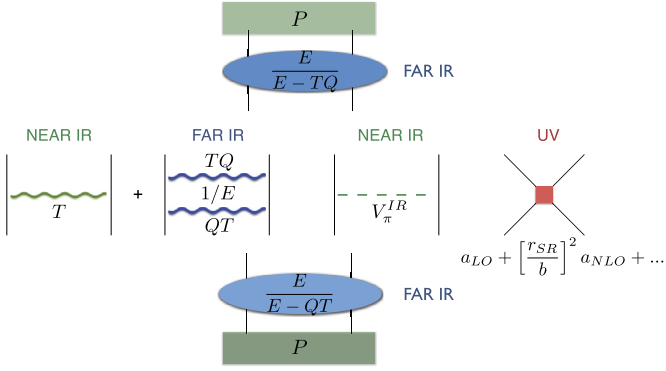


Fig. 1. HOBET’s pionful effective interaction, appropriate to a HO where translational invariance requires P to be defined in terms of total quanta (in contrast to chiral interactions employing a momentum regulator). (Blue, green, red indicate far-IR, near-IR, and UV corrections.)

of HOBET’s LEC is natural and in excellent accord with missing UV physics that can be modeled as a Gaussian hard core of range $a \sim 0.39$ fm, for the specific Argonne v_{18} 1S_0 case studied there.

V_δ impacts the interpretation of the term linear in the potential, written as V in Eq. (1). If we are given a potential V , its short-range contributions will enter in the low-order Talmi integrals, for which there are LECs to fix the values, up to the order of the expansion. That is, one can decompose V into UV and IR components, $V = V^{UV} + V^{IR}$, with V^{UV} denoting the part of V contributing to Talmi integrals where LECs are available, and V^{IR} the remainder. Only V^{IR} is relevant: in any fit to observables, the effects of V^{UV} can be absorbed into the LECs of V_δ .

There are three natural choices for V . In the two-step treatment where V is given, one can treat it as is, knowing only the long-range part V^{IR} will matter. Alternatively, we can sever all connections to V , building a true ET in P , following one of two paths: 1) a pionful ET, with $V \rightarrow V_\pi^{IR}$, building in the correct long-distance NN behavior; or 2) a pionless ET, with $V \rightarrow 0$, in correspondence with pionless EFT [44].

In other EFT approaches pion exchange is frequently treated as an interaction between point nucleons, producing a $1/r^3$ tensor force that must be regulated. That is, the cost of building in the proper long-distance behavior of the NN interaction through an explicit pion is the introduction of a short-range contribution that is both poorly behaved and unrealistic, as the nuclear potential is dominated at short distance by vector mesons, not the pion. In HOBET V is naturally regulated by its embedding in P , and as noted above, operationally plays no role at short range, where LECs are available. For example, in an N^3 LO calculation the leading-order s-wave contribution of V_π – the first Gaussian moment not fixed by an available LEC – is

$$\int r^2 dr r^8 e^{-r^2} V_\pi(r) \sim V_\pi^{IR}.$$

The integrand peaks at $|\vec{r}_1 - \vec{r}_2| \sim 4.1$ fm (taking $b = 1.7$ fm), far out on the tail of the pion exchange potential. Consequently, in the depiction of pionful HOBET of Fig. 1, the term in Eq. (1) linear in V has been replaced with V_π^{IR} and labeled as a near-infrared contribution.

The freedom to extract and cleanly treat only the IR contributions of pion exchange simplifies the treatment of the pion. In approaches where the point-nucleon V_π is treated at all length scales, more complicated pion exchanges must be introduced with increasing order. In HOBET, the relative importance of such contributions decline rapidly with order. Because $V_{2\pi}$ can be well repre-

sented by an effective σ exchange with a mass $m_\sigma \sim 4.7m_\pi$ [45], this can be illustrated by evaluating the relevant Talmi integrals for m_π and m_σ . The contribution of $V_{2\pi}$ relative to V_π drops by a factor ~ 4 per order, as one progresses from LO to N^3 LO. Asymptotically one expects a factor m_σ/m_π . With increasing order the IR correction is pushed to ever larger distances, where the simple V_π dominates. We will discuss HOBET simplified power counting in more detail elsewhere [46].

Lepage plots for these three cases – V^{IR} equated to V_{Av18}^{IR} , V_π^{IR} , and 0 for Argonne v_{18} , pionful HOBET, and pionless HOBET calculations, respectively – are given in Fig. 2, where the fractional error $|\Delta E/E|$ in matrix elements of $V^{eff} \equiv E G_{TQ}(E)(V + V_\delta)E G_{QT}(E)$ are plotted as a function of the sum of the nodal quantum numbers $n + n'$. These are evaluated for the deuteron 3S_1 - 3D_1 bound state at -2.2246 MeV, using $b = 1.7$ fm and $\Lambda_{SM} = 8$. We use the scheme-independent fitting procedure described previously, as that choice cleanly divides the low n, n' matrix elements used in fitting LECs from those of higher n, n' , which are predictions. Only the latter are plotted. The straight lines in the figure are drawn from the fractional error at maximum $n + n' = 10$ to that at minimum $n + n'$ (averaged over the possible values). The steepening of the trajectories with increasing order demonstrates that the improvement is systematic. While the convergence in all three cases is quite satisfactory, the use of scheme-independent fitting in this comparison unduly favors the potential treatment: the proper way to fit the LECs in pionful and pionless HOBET is described below. The steeper trajectories for pionful HOBET shows the advantages of building in our knowledge of the NN interaction’s pion tail. As discussed in [37], the order-by-order convergence of the short-range expansion V_δ , apparent from Fig. 2, is governed by the implicit dimensionless parameter $(r_{SR}/b)^2$, where r_{SR} represents the range of the unresolved short-range physics. In pionful HOBET one would expect r_{SR} to be determined by vector meson or effective sigma masses [45]; in pionless HOBET r_{SR} would be the typical range of the strong interaction.

These plots show that $\mathcal{O}(1)$ errors arise for nodal quantum numbers $n + n' \sim 8$, so that diagonal matrix elements with $n \sim 4$ are not reliable. (Here $n = 1, 2, 3, \dots$) Thus the theory will remain predictive for states whose principal configurations involve excitations with $n = 3$, or $E \sim 4\hbar\omega \sim 60$ MeV, but likely not beyond. This rough estimate of the breakdown scale is in good agreement that deduced from the phase-shift fitting we later describe, where the cost function associated with neglected higher orders in the HOBET expansion selects data $\lesssim 60$ MeV.

The Green’s functions in V^{eff} alter matrix elements only in cases where n or n' resides in the last included shell of P , immediately below Q . All other components of $P|\Psi\rangle$ are annihilated by QT , so that $\frac{E}{E-QT} \rightarrow 1$. We caution that $\frac{E}{E-QT}P|\Psi\rangle$ should not be misconstrued as attaching an IR “tail” to the wave function – that is, as something akin to a Woods-Saxon [47] or J-matrix [48] modification of a HO state. Rather, the Green’s functions are a component of the effective interaction, part of the BH H^{eff} . The P space continues to be the compact HO space described by b and Λ_{SM} – a special space due to its separability.

The remaining terms in Fig. 1, which depend only on T , correct for the effects of HO over-confinement on the kinetic energy. They can be rearranged to form a rescattering series

$$P \left[T + T Q \frac{T}{E} + T Q \frac{T}{E} Q \frac{T}{E} + \dots \right] P = P T \frac{E}{E - QT} P, \quad (8)$$

and summed (see below). The terms generated from QT account for the delocalization that occurs in weakly bound physical states. The shift (relative to the simple HO estimate) grows to $-\hbar\omega$, for a bound state just below threshold.

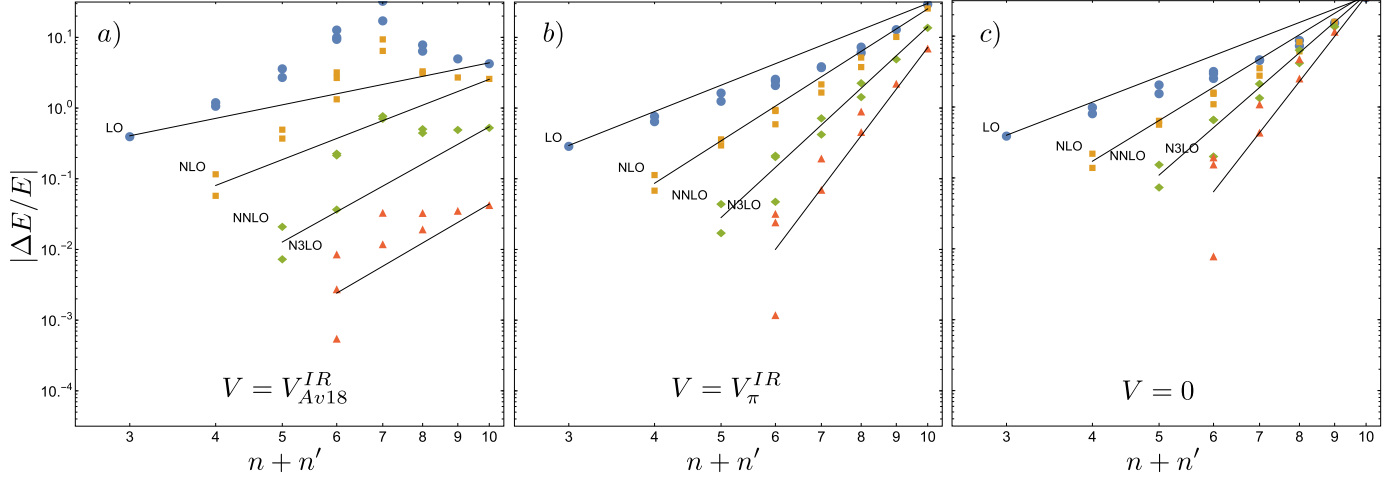


Fig. 2. The Lepage plots for scheme-independent fitting to the s-wave matrix elements of H^{eff} in the deuteron (${}^3S_1 - {}^3D_1$) channel for the Argonne v_{18} potential. The fractional error in V^{eff} is plotted vs. the sum of the nodal quantum numbers. The panels correspond to Eq. (1) with a) $V = V_{Av18}^{IR}$; b) $V = V_{\pi}^{IR}$ (pionful HOBET), and c) $V = 0$ (pionless HOBET). See text.

The edge state can be computed from the free Green's function, at the cost of a matrix inversion in P

$$EG_{QT}P|n\ell m\rangle = G_0(E)[PG_0(E)P]^{-1}|n\ell m\rangle, \\ G_0(E) = \begin{cases} 1/(\nabla^2 - \kappa^2) & E < 0 \\ 1/(\nabla^2 + k^2) & E > 0. \end{cases} \quad (9)$$

A homogeneous term $\phi(E)$ can be added on the right, a freedom we will exploit to build in the correct boundary conditions for our continuum states. Here $\kappa \equiv \sqrt{2|E|/\hbar\omega}$, $k = \sqrt{2E/\hbar\omega}$, and ∇ are dimensionless. Matrix elements of G_0 in P can be evaluated analytically. We employ standing-wave Green's functions.

The proper treatment of these Green's functions is important to our main goal, a consistent one-step procedure for determining HOBET's H^{eff} directly from scattering data, rather than through the two-step process of constructing then renormalizing a potential.

In the case of bound states, as described in earlier work [37], self-consistent solutions of the BH equation are obtained only at the eigenvalues E , for a given choice of LECs. $G_0(E)$ depends only on E . Thus if an eigenvalue E is known – the simplest example is the deuteron bound state – one should demand a solution at that E . This becomes an implicit constraint on the LECs. Just as the deuteron binding energy is used in parameterizations of conventional potentials, the LEC $a_{l0}^{3S_1}$ can be determined by demanding a BH solution at $E = -2.2246$ MeV.

However, most of our information on the NN interaction comes from phase shifts and mixing angles, and thus from continuum states. HOBET treats bound and continuum states on an equal footing, in each case generating the restrictions of the full wave functions to P . Unlike the bound-state case with discrete eigenvalues, there exists a solution at every energy $E > 0$. The self-consistency constraint now comes from the fact that the Green's function depends not only on E , but also the phase shift $\delta_\ell(E)$. The experimental phase shift is used directly in the nuclear H^{eff} , inserted through the homogeneous term in the kinetic energy Green's function, rather than in a nucleon-level potential,

$$G_0^\ell(E > 0, \delta_\ell(E); \mathbf{r}, \mathbf{r}') = -\frac{\cos k|\mathbf{r} - \mathbf{r}'|}{4\pi|\mathbf{r} - \mathbf{r}'|} \\ - k \cot \delta_\ell(E) j_\ell(kr) j_\ell(kr') \sum_m Y_{\ell m}(\Omega) Y_{\ell m}^*(\Omega'). \quad (10)$$

When the resulting H^{eff} is diagonalized, in general an eigenvalue at the selected E will not be found. As the theory is complete and the IR behavior correct, the source of this discrepancy must be in the UV, an inadequate V_δ . V_δ 's LECs should then be adjusted to fix the discrepancy.

LECs are chosen to produce a best fit to all of the phase shift information from threshold to a “fuzzy” maximum in the CM energy, through the procedure described below. The relevant experimental information depends on the order of the HOBET expansion and the choice of P space. For N³LO and the P used in our study ($\Lambda_{\text{SM}} = 8$, $b = 1.7$ fm), the relevant data correspond to CM energies $\lesssim 50$ MeV. The channels that enter at N³LO are 1S_0 , ${}^3S_1 - {}^3D_1$, 1D_2 , 3D_1 , 3D_2 , ${}^3D_3 - {}^3G_3$, 1P_1 , 3P_0 , 3P_1 , ${}^3P_2 - {}^3F_2$, 1F_3 , 3F_3 and 3F_4 . The number of LECs at N³LO varies from six in the S-wave channels to one in the F-wave and mixed DG-wave channels. In these fits V_π with pion mass dependence is taken from Eq. 17, 18 and 19 of [2] using the recommended coupling constant value $f^2 = 0.075$. Smaller intermediate range contributions from Eq. 20 in the same paper corresponding to two pion exchange have been omitted. The regulator $(1 - e^{-cr^2})$ has also been removed as the potential is automatically regulated by the P -space basis. As a crosscheck on this procedure, N³LO LEC fits were also done in the 1F_3 channel with phase shifts at 2, 5, 10, 15, 20, 25, 30, 40, and 50 MeV in which f^2 was treated as a second LEC, together with the N³LO LEC. The fit yielded a very similar value $f^2 = 0.074$, demonstrating numerically that pion exchange dominates the NN potential at the long distances where V_π^{IR} contributes.

Before we tackled the fitting of LECs with experimental phase shifts, we performed a numerical experiment with an analytic S-wave model – a square well plus hard core resembling the nuclear potential – for which exact scattering parameters can be derived. This experiment influenced the procedures we designed. We solved for H^{eff} using a HOBET P space with $b = 1.7$ fm and $\Lambda = 8$ (5 included S-states). Rapid convergence was found, a \sim two-orders-of-magnitude improvement in χ^2 per order in the expansion [46]. We then did a series of calculations to explore the consequences of omitted higher-order operators on the LECs of retained, lower-order operators. First, we worked through a set of 10 energies E_i equally space from 1 to 10 MeV, using a Green's function with the appropriate model phase shifts at the E_i , solving for a_{l0} by requiring $H^{\text{eff}}(E_i)$ to have eigenvalue E_i . The ten values we obtained are shown as the upper blue dots in Fig. 3: a slight energy dependence in the determined a_{l0} is apparent, about 3% over the energy range.

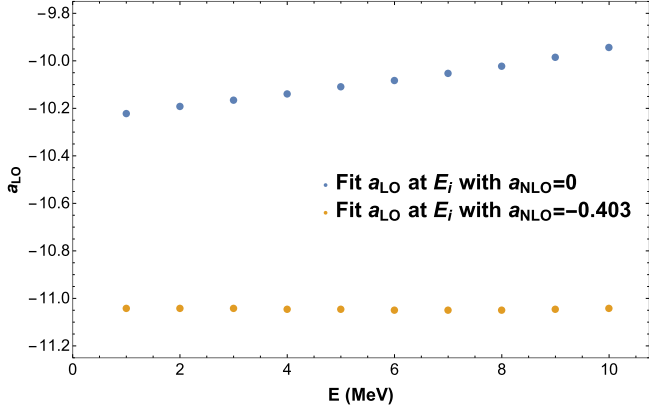


Fig. 3. Energy dependence of a_{LO} at LO (upper dots) and residual energy dependence a_{LO} at NLO (lower dots) after a_{NLO} is fixed at -0.403 .

Second, we then repeated the fit at two energies E_i , 1 and 10 MeV, but at NNLO, adjusting a_{LO} and a_{NLO} so that again the $H^{eff}(E_i)$ yielded E_i . Third, keeping a_{NLO} fixed at the value determined in the second step, we repeated the initial set of LO calculations. The resulting a_{LO} s, shown as the lower gold dots in Fig. 3, now exhibit almost no dependence on energy ($< 0.1\%$).

This and other experiments provided strong evidence the average effect of omitted higher-order operators is to a very good approximation absorbed by the operators of the last included order. This allows us to simplify the fitting of LECs in high-order calculation, through a bootstrap or iterative procedure. For example, for a fit at the NNLO, the LO LECs can be taken from the previous NLO fit and held fixed; only the NLO and NNLO LECs need to be fit, with previously determined values for the NLO LECs serving as reasonable initial values. In a subsequent N^3LO fit, the LO and NLO LECs would be kept fixed at the values determined in the NNLO calculation, with only the NNLO and N^3LO terms adjusted.

We then applied this procedure to realistic NN scattering. The phase shifts and mixing angles we use in testing our procedure are those generated from Argonne v_{18} . Because the potential's parameters are carefully fit to scattering data, numerically these phase shifts can be regarded as experimental ones. But unlike experiment data with errors, this gives us a potential and a set of scattering data that are precisely equivalent at each energy, which is helpful for some of the tests we describe below.

Several interesting issues that arise in the fitting procedure are described in detail elsewhere [49], and thus are treated briefly here. Given a potential and a consistent set of scattering data, one can compare the scheme-independent LEC fitting procedure of [37] with the new procedure described above. In the earlier procedure, individual matrix elements of H^{eff} were calculated numerically from Argonne v_{18} , with a_{LO} then determined from the $1s-1s$ matrix element, etc. We found that the H^{eff} determined with the current scheme does a significantly better job in representing scattering data [49] than the earlier scheme-independent method. We attribute this to the ability of the new fit, through the last included order, to absorb the average effects of omitted higher-order operators.

The fitting is done at selected continuum energies (or equivalently momenta); in the case of the $^3S_1-^3D_1$ channel, one can also choose to use the bound state. What grid of points should be used in fits? The resolution of unity in the channel $|l, m\rangle$ is

$$1 = \sum_{i \in \text{bound}} |i \ell m\rangle \langle i \ell m| + \frac{2}{\pi} \int_0^\infty dk |k \ell m\rangle \langle k \ell m| \quad (11)$$

$$\langle r | k \ell m\rangle \equiv kr [-\cos \delta_{\ell j_\ell}(kr) + \sin \delta_{\ell j_\ell}(kr)].$$

As the integral is weighted in dk , not in dE , we select points evenly spread in k . (Note that with experimental data or phase shifts obtained from lattice QCD calculations, we would not have this freedom, and thus a more sophisticated weighting of points might be needed.)

The number of sample points must at a minimum exceed the number of LECs to be fit: in practice considerably more are used. The adequacy of the continuum grid selected can be checked by increasing the density of points to verify that consistent LECs are obtained.

What range of continuum momenta should be used in the fit, and how should grid points be weighted? Generally the LECs of an ET for some low-energy P are determined from the longest wavelength information available. If the ET is well behaved, then once its LECs are determined, other long-wavelength observables can be predicted, including those somewhat beyond the momentum or energy scale used in the LEC fitting. Intuitively one anticipates that a LO theory would utilize very long wavelength information in its LEC fitting, and be valid only over a limited range of energies or momenta. Additional input at somewhat shorter wavelengths would be needed to determine the LECs of a NLO theory, and the resulting ET would be valid over a somewhat more extended range, and so on. Our LEC fitting procedure is designed to emphasize data from an energy range appropriate to the order of the fit being done.

This is accomplished through a cost function that takes into account the potential impact of operators beyond the order being considered. Fits are done over a set of energies substantially larger than the number of LECs being determined. With an exact ET and perfect phase shift data, $PH^{eff}(E_i)P|\Psi_i\rangle = E_iP|\Psi_i\rangle$ for each energy E_i of a set spanning the energy interval of interest. But as the ET is only executed to some specified order N , $PH^{eff}(E_i)P|\Psi_i\rangle = \epsilon_i^N P|\Psi_i\rangle$, where ϵ_i^N is an eigenvalue near but not identical to E_i . We determine the LECs by minimizing the cost function

$$\chi_{\text{order } N}^2 = \sum_{i \in \{\text{sample}\}} \frac{(\epsilon_i^N - E_i)^2}{\sigma_{N+1}(i)^2}, \quad (12)$$

where $\{\text{sample}\}$ represents the set of energy points used, in the case of unmixed channels such as 1S_0 and 3P_0 .

The variance σ_i^2 is an estimate of the contributions of omitted higher-order LECs not included in the fit,

$$\sigma_{N+1}^2(i) \sim \kappa_{N+1}^2 \sum_{\{a_j^{N+1}\}} \left(\left. \frac{\partial \epsilon_i^{N+1}}{\partial a_j^{N+1}} \right|_{a_j^{N+1}=0} \right)^2. \quad (13)$$

Here ϵ_i^{N+1} is the eigenvalue at one order beyond that being employed in the fit, and $\{a_j^{N+1}\}$ is the set of LECs that contribute in that order. Under the assumption that the values of these LECs are uncorrelated, the change in the energy $(\epsilon_i^N - E_i)^2$ that would result from turning on the $\{a_j^{N+1}\}$ can be estimated from the sum over the squares of first-derivative variations in each of the directions a_j^{N+1} , evaluated at $a_j^{N+1} = 0$. These would then be folded with an estimate of the typical scale of such variations, represented by κ_{N+1}^2 in Eq. (13), which in a direct calculation at order $N+1$ would be computable from the values obtained for the LECs for order $N+1$. Absent such a calculation, κ_{N+1}^2 can be estimated from the lower-order LECs, under the assumption of naturalness. In the present treatment, the value of κ_{N+1}^2 is irrelevant, as it acts a common scale factor in $\chi_{\text{order } N}^2$, and thus does not alter the relative weightings of energy points in our sample. (This would not be the case were we fitting experimental phase shifts with errors,

Table 1

Deuteron channel: binding energy E_b as a function of the expansion order. Bare denotes a calculation with $T + V_{IR}$ and no IR correction. The error columns are the average of squared fractional error up to 10 MeV.

Order	E_b^{pionless}	Error	E_b^{pionful}	Error
bare	3.0953	-	-0.67187	-
LO	-0.9214	1.16E-2	-2.0206	1.84E-3
NLO	-1.5392	1.53E-3	-2.17814	3.44E-5
NNLO	-1.6267	1.37E-3	-2.1952	3.32E-5
N ³ LO	-2.0690	1.34E-4	-2.2278	6.07E-6

as Eq. (13) would then include a second term reflecting those errors – an uncertainty in the energy to which one should assign an experimental phase shift.)

In the LEC fitting, the $\sigma_{N+1}^2(i)$ generate a soft cutoff in the energies over which we sample. In a LO calculation, a high weight is placed on energy points where the NLO contribution is expected to be small, and a low weight on those where the NLO contribution is large; σ_i^2 increases as the energy E_i is raised. The net effect of the resulting cost function is to limit the range of contributing phase shifts to low energies. The range grows with increasing order, reflecting the greater importance of higher energy scattering data to higher order LECs.

Numerically it proved helpful to perform fits successively, e.g., with the final results for the NLO LECs used as the starting values in the search for the best values of N²LO LECs, and so on. This improves the rate of convergence in higher orders, where the cost function minimization is over multiple LECs [49].

The above discussion applies to single channels: in mixed channels, such as ${}^3S_1-{}^3D_1$, one obtains for a given energy E_i two standing-wave solutions, which due to the typically small mixing value Σ will be mostly S channel and mostly D channel,

$$\begin{aligned} |\Psi_S\rangle &= \cos \Sigma |S(\delta_S)\rangle - \sin \Sigma |D(\delta_S)\rangle, \\ |\Psi_D\rangle &= \sin \Sigma |S(\delta_D)\rangle + \cos \Sigma |D(\delta_D)\rangle, \end{aligned} \quad (14)$$

with the indicated phase shifts, where the notation corresponds to the Blatt-Biedenharn [50] parameterization of the S-matrix

$$\hat{S} = \hat{O}^{-1} \begin{pmatrix} e^{2i\delta_S} & 0 \\ 0 & e^{2i\delta_D} \end{pmatrix} \hat{O}, \quad \hat{O} = \begin{pmatrix} \cos \Sigma & -\sin \Sigma \\ \sin \Sigma & \cos \Sigma \end{pmatrix}. \quad (15)$$

The general standing wave solution can be written as a mixture of the basis states given in Eq. (14), with probabilities $\cos^2 \alpha$ and $\sin^2 \alpha$ for $|\Psi_S\rangle$ and $|\Psi_D\rangle$, respectively. The single-channel sampling is generalized for mixed channels by including in the sampling not only grid points in k , but values α of 0, $\frac{\pi}{4}$, and $\frac{\pi}{2}$ at each k . This allows us to access the three degrees of freedom in the S-matrix, δ_S , δ_D , and Σ . Details are given in [49].

We then applied our procedures to our Argonne v_{18} -equivalent scattering database, for both pionful and pionless HOBET. For fitting 41 phase shift data samples are used, evenly spaced in k , and running from 1.0 to 80.0 MeV. 80 MeV is well beyond the point where N⁴LO LECs are needed and demonstrates the effectiveness of the soft cutoff created by σ_{N+1}^2 . In the coupled channel case if $\cot \delta_D > 100.0$ we drop the sample for numerical reasons in the construction of the Green's function for G_{QT} . By carrying out the fitting program from LO through N³LO, we obtained a series of LEC sets defining a progression of HOBET potentials of increasing sophistication. The ${}^3S_1-{}^3D_1$ deuteron bound-state energy was not included in the fitting, and therefore becomes a prediction. Table 1 shows the results as a function of order.

While both pionful and pionless calculations converge well, the comparison shows the importance of the including the pion, which

Table 2

The deuteron channel and S-wave LECs determined at N³LO in pionless and pionful HOBET. See [46] for the full set of couplings.

Transitions	LECs (MeV)	Pionless	Pionful
${}^3S_1 \leftrightarrow {}^3S_1$	a_{LO}^{3S1}	-50.9105	-47.2779
	a_{NLO}^{3S1}	-4.3625	-5.1453
	$a_{NNLO}^{3S1,22}$	1.8670E-2	-9.6852E-1
	$a_{NNLO}^{3S1,40}$	-2.2203E-1	-2.4459E-1
	$a_{NNLO}^{3S1,42}$	2.3691E-2	-1.3784E-1
	$a_{N3LO}^{3S1,60}$	-6.7398E-2	-4.7928E-2
${}^3S_1 \leftrightarrow {}^3D_1$	a_{NLO}^{SD}	-2.6731	-9.4681
	$a_{NNLO}^{SD,22}$	-6.8852E-1	-3.0647
	$a_{NNLO}^{SD,04}$	3.4194E-1	-1.4228
	$a_{NNLO}^{SD,42}$	-7.3097E-2	-4.8398E-1
	$a_{N3LO}^{SD,24}$	-2.3028E-2	-7.3943E-1
	$a_{N3LO}^{SD,06}$	9.1250E-2	-5.3541E-2
${}^3D_1 \leftrightarrow {}^3D_1$	a_{NNLO}^{3D1}	4.5685	3.2278
	a_{N3LO}^{3D1}	8.7938E-1	9.1347E-1
${}^1S_0 \leftrightarrow {}^1S_0$	a_{LO}^{1S0}	-38.5612	-38.5364
	a_{NLO}^{1S0}	-5.7331	-5.9948
	$a_{NNLO}^{1S0,22}$	-8.8427E-1	-1.2224
	$a_{NNLO}^{1S0,40}$	-3.9656E-1	-4.2192E-1
	$a_{NNLO}^{1S0,42}$	-6.5638E-2	-1.5812E-1
	$a_{N3LO}^{1S0,60}$	-3.8120E-2	-4.1352E-2

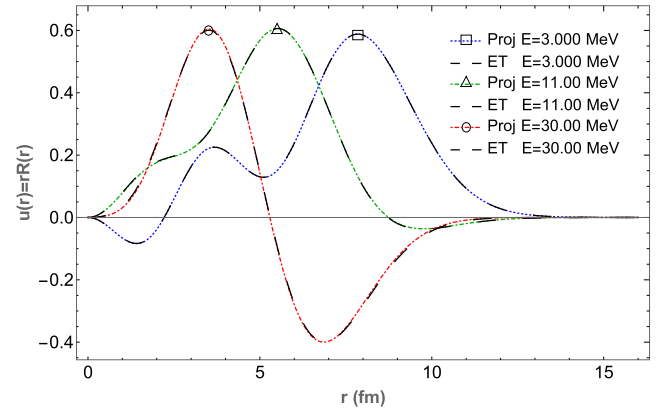


Fig. 4. Projections of exactly computed 1P_1 relative wave functions (colored, dotted lines) are shown to match the HOBET wave functions (large black dashes) nearly perfectly, for representative continuum energies. The results are predictions: the selected energies are distinct from those used in LEC fitting.

we stress again is explicitly an IR correction in HOBET. At N³LO the deuteron binding energy is correct to 3 keV, and the phase-shift fit (reflected in the self-consistency error) is nearly perfect. Table 2 gives the N³LO ${}^3S_1-{}^3D_1$ and 1S_0 LECs obtained; results for other channels can be found in [46].

We also compared the HOBET 1P_1 wave functions to projections of the exactly computed wave functions at energies 3, 11, and 30 MeV, which were deliberately chosen to be distinct from the sample energies 2.55, 3.22, 10.14, 11.45, 28.83, and 31.0 MeV, to ensure that results are not directly constrained by our fitting. Fig. 4 shows that the wave functions are in nearly perfect agreement: all of the detailed behavior of the projected wave functions as continuous functions of r and E , remarkably, can be encoded in a few energy-independent LECs, provided the leading energy dependence is first treated via the QT summation of Eq. (1).

Once HOBET's LECs are fixed, phase shifts can be predicted as continuous functions of E : With E held constant, one finds the

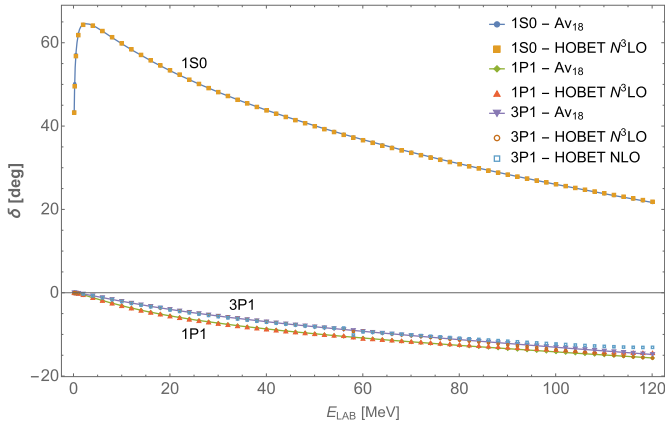


Fig. 5. Phase shifts are generated from the $N^3\text{LO}$ LECs in the 1S_0 (6 LECs), and 1P_1 (4 LECs), 3P_1 (4 LECs) channels and compared to phase shifts derived from AV_{18} . Even the 3P_1 NLO fit yields good convergence.

phase-shift that produces a self-consistent energy eigenvalue. The 1S_0 , 1P_1 , and 3P_1 phase shifts are shown in Fig. 5.

The HOBET formalism connecting LECs to phase shifts is based on an exact reorganization of the BH equation to isolate the important IR corrections to H^{eff} that arise from the coupling of P and Q by T . HOBET's QT summation removes this coupling, thus restoring the scale separation necessary for a well-behaved EFT [34–36]. This procedure establishes a direct connection between the LECs of HOBET's H^{eff} and the phase shifts experimentalists measure. Other procedures to connect confined HO wave functions to phase shifts have been explored recently. These alternatives generally take matrix elements of a momentum basis EFT interaction in the HO basis, preserving the LECs. An early example fits the LECs to binding energies of light nuclei [51]. In more recent examples the LECs are tuned to reproduce continuum phase shifts obtained via the J-matrix method [48]. A pion-less EFT example is developed by Binder et al. using the kinetic energy eigenstates, known as a DVR basis, in P for matching [52]. A chiral EFT example is also developed by Yang [53], in which he finds (for a P comparable to that we use here) that the J-matrix method induces large $\mathcal{O}(1)$ oscillations in the predicted phase shifts, in contrast to Fig. 4. These oscillations can be damped by using very large P spaces, but remain apparent even at $\Lambda_{SM} \sim 60$. In a follow-on paper to Binder et al., oscillations of the P -space potential away from the matching points at low k are suppressed by adjusting the weight of the highest k DVR state in the P -space potential and the improvement is demonstrated for a contact interaction [54]. A major distinction between these approaches and HOBET is that the renormalization impact of kinetic energy explicitly handled in HOBET is left for extrapolation in Λ_{SM} , requiring the use of larger model spaces.

In summary, we have demonstrated a precise method to construct the effective interaction needed at the nuclear scale, directly from experimental phase shifts. The only regulators that enter in this one-step method are those defining the soft nuclear Hilbert space P itself, namely b and Λ_{SM} . Thus one can avoid the usual procedure in which scattering data are first encoding in a high-momentum potential, then decoded through a series of potential softening and renormalization steps, with associated approximations. The method exploits HOBET's explicit continuity in energy, which allows one to connect NN scattering information at a specified energy to the properties of a bound state at a different energy, without approximations. The pionless and pionful theories both converge at the nuclear momentum scale, with the pionful theory producing a $N^3\text{LO}$ deuteron binding energy accurate to ~ 3 keV.

HOBET generates not only exact eigenvalues (to the tolerance achieved in the expansion) but also wave functions that corre-

spond to the exact projections of bound or continuum states to P . Such wave functions evolve simply with changes in P , e.g., an increase in Λ_{SM} simply adds new components to the wave function, leaving others unchanged. While HOBET's convergence can be slowed by picking a non-optimal P , observables are independent of this choice, provided the expansion is carried out to the requisite order. That is, answers are independent of the regulators b and Λ_{SM} . These various properties are attractive in an ET.

Work is underway on key extensions of this formalism [46]:

1. A precise connection between nuclear properties and scattering data has important implications for relating nonrelativistic nuclear structure to lattice QCD (LQCD). Phase shifts calculated from LQCD [55–57] can be used directly in our HOBET method, with the match determining HOBET's LECs. But one can do this matching at a more primitive level, using the LQCD eigenvalues in a finite rectangular volume, by confining HOBET to the same volume. There are important advantages to doing this. The method exploits the attractive transformation properties of HO wave functions between Cartesian and spherical bases.
2. The interaction derived here can be directly embedded in more complex nuclei. Three-body corrections, which we expect to be significant given the small P spaces we use ($\Lambda_{SM} = 8$), can be determined from experimental data such as the $A = 3$ binding and pD scattering. An important motivation for HOBET is that a cluster expansion of the strong interaction should converge rapidly in the number of interacting nucleons, if they are unfolded from the IR corrections, as has been done in the two-nucleon case.
3. Our Talmi integral discussion touches on the “power counting” contrasts between HOBET and plane-wave EFT treatments that include the point-nucleon V_π and corrections at all ranges. A much more detailed discussion is warranted.

Acknowledgements

This material is based upon work supported in part by the US Department of Energy, Office of Science, Office of Nuclear Physics and SciDAC under awards DE-SC00046548, DE-AC02-05CH11231, KB0301052, and DE-SC0015376. We thank Christian Drischler for helpful discussions.

References

- [1] R. Machleidt, Phys. Rev. C 63 (2) (2001) 024001, <https://doi.org/10.1103/PhysRevC.63.024001>.
- [2] R.B. Wiringa, V.G.J. Stoks, R. Schiavilla, Phys. Rev. C 51 (1) (1995) 38–51, <https://doi.org/10.1103/PhysRevC.51.38>.
- [3] S.C. Pieper, R.B. Wiringa, Annu. Rev. Nucl. Part. Sci. 51 (1) (2001) 53–90, <https://doi.org/10.1146/annurev.nucl.51.101701.132506>.
- [4] J.J. de Swart, R.A.M.M. Klomp, M.C.M. Rentmeester, T.A. Rijken, in: *Few-Body Systems Suppl.*, vol. 8, Springer-Verlag, 1995, pp. 438–447.
- [5] R. Machleidt, D. Entem, Phys. Rep. 503 (1) (2011) 1–75, <https://doi.org/10.1016/j.physrep.2011.02.001>.
- [6] E. Epelbaum, H.-W. Hammer, U.-G. Meißner, Rev. Mod. Phys. 81 (4) (2009) 1773–1825, <https://doi.org/10.1103/RevModPhys.81.1773>.
- [7] E. Epelbaum, A. Nogga, W. Glöckle, H. Kamada, U.-G. Meißner, H. Witała, Phys. Rev. C 66 (6) (2002) 064001, <https://doi.org/10.1103/PhysRevC.66.064001>.
- [8] H.A. Bethe, Phys. Rev. 103 (5) (1956) 1353–1390, <https://doi.org/10.1103/PhysRev.103.1353>.
- [9] T.T.S. Kuo, G.E. Brown, Nucl. Phys. 85 (1) (1966) 40–86, [https://doi.org/10.1016/0029-5582\(66\)90131-3](https://doi.org/10.1016/0029-5582(66)90131-3).
- [10] B.R. Barrett, M.W. Kirson, Nucl. Phys. A 148 (1) (1970) 145–180, [https://doi.org/10.1016/0375-9474\(70\)90617-2](https://doi.org/10.1016/0375-9474(70)90617-2).
- [11] T. Schucan, H. Weidenmüller, Ann. Phys. 73 (1) (1972) 108–135, [https://doi.org/10.1016/0003-4916\(72\)90315-6](https://doi.org/10.1016/0003-4916(72)90315-6).
- [12] T.H. Schucan, H.A. Weidenmüller, Ann. Phys. 76 (2) (1973) 483–509, [https://doi.org/10.1016/0003-4916\(73\)90044-4](https://doi.org/10.1016/0003-4916(73)90044-4).
- [13] M.I. Haftel, F. Tabakin, Phys. Rev. C 3 (2) (1971) 921–936, <https://doi.org/10.1103/PhysRevC.3.921>.

- [14] J. Côté, B. Rouben, R. De Tourreil, D. Sprung, Nucl. Phys. A 273 (2) (1976) 269–285, [https://doi.org/10.1016/0375-9474\(76\)90591-1](https://doi.org/10.1016/0375-9474(76)90591-1).
- [15] S. Bogner, National nuclear physics summer school online talks, Chapel Hill, 2011, <http://www.int.washington.edu/NNPSS/talks.html>.
- [16] A. Nogga, S.K. Bogner, A. Schwenk, Phys. Rev. C 70 (6) (2004) 061002, <https://doi.org/10.1103/PhysRevC.70.061002>.
- [17] S. Bogner, R. Furnstahl, S. Ramanan, A. Schwenk, Nucl. Phys. A 773 (3–4) (2006) 203–220, <https://doi.org/10.1016/j.nuclphysa.2006.05.004>.
- [18] S. Bogner, A. Schwenk, R. Furnstahl, A. Nogga, Nucl. Phys. A 763 (2005) 59–79, <https://doi.org/10.1016/j.nuclphysa.2005.08.024>.
- [19] S. Bogner, R. Furnstahl, Phys. Lett. B 632 (4) (2006) 501–506, <https://doi.org/10.1016/j.physletb.2005.10.094>.
- [20] S. Bogner, R. Furnstahl, Phys. Lett. B 639 (3–4) (2006) 237–241, <https://doi.org/10.1016/j.physletb.2006.06.037>.
- [21] S.D. Glazek, K.G. Wilson, Phys. Rev. D 49 (8) (1994) 4214–4218, <https://doi.org/10.1103/PhysRevD.49.4214>.
- [22] S.D. Glazek, K.G. Wilson, Phys. Rev. D 48 (12) (1993) 5863–5872, <https://doi.org/10.1103/PhysRevD.48.5863>.
- [23] S.K. Bogner, R.J. Furnstahl, R.J. Perry, Phys. Rev. C 75 (6) (2007) 061001, <https://doi.org/10.1103/PhysRevC.75.061001>.
- [24] E.D. Jurgenson, S.K. Bogner, R.J. Furnstahl, R.J. Perry, Phys. Rev. C 78 (1) (2008) 014003, <https://doi.org/10.1103/PhysRevC.78.014003>.
- [25] H. Hergert, S. Bogner, T. Morris, A. Schwenk, K. Tsukiyama, Phys. Rep. 621 (2016) 165–222, <https://doi.org/10.1016/j.physrep.2015.12.007>.
- [26] J.D. Holt, T.T. Kuo, G.E. Brown, Phys. Rev. C, Nucl. Phys. 69 (3) (2004) 034329, <https://doi.org/10.1103/PhysRevC.69.034329>.
- [27] P. Navrátil, J.P. Vary, B.R. Barrett, Phys. Rev. C 62 (5) (2000) 054311, <https://doi.org/10.1103/PhysRevC.62.054311>.
- [28] P. Navrátil, S. Quaglioni, I. Stetcu, B.R. Barrett, J. Phys. G, Nucl. Part. Phys. 36 (8) (2009) 083101, <https://doi.org/10.1088/0954-3899/36/8/083101>.
- [29] C.W. Johnson, W.E. Ormand, K.S. McElvain, H. Shan, arXiv:1801.08432.
- [30] D.J. Dean, M. Hjorth-Jensen, Phys. Rev. C 69 (5) (2004) 054320, <https://doi.org/10.1103/PhysRevC.69.054320>.
- [31] G. Hagen, T. Papenbrock, M. Hjorth-Jensen, D.J. Dean, Rep. Prog. Phys. 77 (9) (2014) 096302, <https://doi.org/10.1088/0034-4885/77/9/096302>.
- [32] Ø. Jensen, G. Hagen, T. Papenbrock, D.J. Dean, J.S. Vaagen, Phys. Rev. C 82 (1) (2010) 014310, <https://doi.org/10.1103/PhysRevC.82.014310>.
- [33] W.C. Haxton, C.-L. Song, Phys. Rev. Lett. 84 (24) (2000) 5484–5487, <https://doi.org/10.1103/PhysRevLett.84.5484>.
- [34] W. Haxton, T. Luu, Nucl. Phys. A 690 (1–3) (2001) 15–28, [https://doi.org/10.1016/S0375-9474\(01\)00927-7](https://doi.org/10.1016/S0375-9474(01)00927-7).
- [35] W.C. Haxton, T. Luu, Phys. Rev. Lett. 89 (18) (2002) 182503, <https://doi.org/10.1103/PhysRevLett.89.182503>.
- [36] T.C. Luu, S. Bogner, W.C. Haxton, P. Navrátil, Phys. Rev. C 70 (1) (2004) 014316, <https://doi.org/10.1103/PhysRevC.70.014316>.
- [37] W.C. Haxton, Phys. Rev. C 77 (3) (2008) 034005, <https://doi.org/10.1103/PhysRevC.77.034005>.
- [38] C. Bloch, J. Horowitz, Nucl. Phys. B 8 (1958) 91–105, [https://doi.org/10.1016/0029-5582\(58\)90136-6](https://doi.org/10.1016/0029-5582(58)90136-6).
- [39] B.K. Jennings, Europhys. Lett. 72 (2) (2005) 211–215, <https://doi.org/10.1209/epl/i2005-10215-y>.
- [40] B.H. Brandow, Rev. Mod. Phys. 39 (4) (1967) 771–828, <https://doi.org/10.1103/RevModPhys.39.771>.
- [41] S. Lee, K. Suzuki, Phys. Lett. B 91 (2) (1980) 173–176, [https://doi.org/10.1016/0370-2693\(80\)90423-2](https://doi.org/10.1016/0370-2693(80)90423-2).
- [42] K. Suzuki, S.Y. Lee, Prog. Theor. Phys. 64 (6) (1980) 2091–2106, <https://doi.org/10.1143/PTP.64.2091>.
- [43] A. de Shalit, I. Talmi, Nuclear Shell Theory, Academic Press Inc., New York, London, 1963.
- [44] J.-W. Chen, G. Rupak, M.J. Savage, Nucleon-nucleon effective field theory without pions, Nucl. Phys. A 653 (4) (1999) 386–412, [https://doi.org/10.1016/S0375-9474\(99\)00298-5](https://doi.org/10.1016/S0375-9474(99)00298-5).
- [45] S. Oshima, T. Fujita, N. Kanda, A. Yoshimi, J. Mod. Phys. 06 (07) (2015) 927–936, <https://doi.org/10.4236/jmp.2015.67097>.
- [46] K.S. McElvain, W.C. Haxton, in preparation.
- [47] R.D. Woods, D.S. Saxon, Phys. Rev. 95 (2) (1954) 577–578, <https://doi.org/10.1103/PhysRev.95.577>.
- [48] A.D. Alhaidari, E.J. Heller, H.A. Yamani, M.S. Abdelmonem, The J-Matrix Method: Developments and Applications, Springer Netherlands, Dordrecht, 2008.
- [49] K.S. McElvain, Harmonic Oscillator Based Effective Theory, Connecting LQCD to Nuclear Structure, Ph.D. thesis, University of California, Berkeley, 2017, <https://escholarship.org/uc/item/1vj4x39c>.
- [50] J.M. Blatt, L.C. Biedenharn, Phys. Rev. 86 (3) (1952) 399–404, <https://doi.org/10.1103/PhysRev.86.399>.
- [51] I. Stetcu, B.R. Barrett, U. van Kolck, Phys. Lett. B 653 (2–4) (2007) 358–362, <https://doi.org/10.1016/j.physletb.2007.07.065>.
- [52] S. Binder, A. Ekström, G. Hagen, T. Papenbrock, K.A. Wendt, Phys. Rev. C 93 (4) (2016) 044332, <https://doi.org/10.1103/PhysRevC.93.044332>.
- [53] C.J. Yang, Phys. Rev. C 94 (6) (2016) 1–9, <https://doi.org/10.1103/PhysRevC.94.064004>.
- [54] A. Bansal, S. Binder, A. Ekström, G. Hagen, G.R. Jansen, T. Papenbrock, Phys. Rev. C 98 (5) (2018) 52–54, <https://doi.org/10.1103/PhysRevC.98.054301>.
- [55] E. Berkowitz, T. Kurth, A. Nicholson, B. Joó, E. Rinaldi, M. Strother, P.M. Vranas, A. Walker-Loud, Phys. Lett. B 765 (2017) 285–292, <https://doi.org/10.1016/j.physletb.2016.12.024>.
- [56] S.R. Beane, E. Chang, S.D. Cohen, W. Detmold, P. Junnarkar, H.W. Lin, T.C. Luu, K. Orginos, A. Parreño, M.J. Savage, A. Walker-Loud, Phys. Rev. C 88 (2) (2013) 024003, <https://doi.org/10.1103/PhysRevC.88.024003>.
- [57] K. Murano, N. Ishii, S. Aoki, T. Doi, T. Hatsuda, Y. Ikeda, T. Inoue, H. Nemura, K. Sasaki, Phys. Lett. B 735 (2014) 19–24, <https://doi.org/10.1016/j.physletb.2014.05.061>.